



A Novel HER3-Targeting Antibody–Drug Conjugate, U3-1402, Exhibits Potent Therapeutic Efficacy through the Delivery of Cytotoxic Payload by Efficient Internalization

Yuuri Hashimoto¹, Kumiko Koyama¹, Yasuki Kamai¹, Kenji Hirotsu¹, Yusuke Ogitani¹, Akiko Zembutsu¹, Manabu Abe¹, Yuki Kaneda¹, Naoyuki Maeda¹, Yoshinobu Shiose¹, Takuma Iguchi¹, Tomomichi Ishizaka¹, Tsuyoshi Karibe¹, Ichiro Hayakawa¹, Koji Morita¹, Takashi Nakada¹, Taisei Nomura², Kenichi Wakita¹, Takashi Kagari¹, Yuki Abe¹, Masato Murakami¹, Suguru Ueno¹, and Toshinori Agatsuma¹

Abstract

Purpose: HER3 is a compelling target for cancer treatment; however, no HER3-targeted therapy is currently clinically available. Here, we produced U3-1402, an anti-HER3 antibody–drug conjugate with a topoisomerase I inhibitor exatecan derivative (DXd), and systematically investigated its targeted drug delivery potential and antitumor activity in preclinical models.

Experimental Design: *In vitro* pharmacologic activities and the mechanisms of action of U3-1402 were assessed in several human cancer cell lines. Antitumor activity of U3-1402 was evaluated in xenograft mouse models, including patient-derived xenograft (PDX) models. Safety assessments were also conducted in rats and monkeys.

Results: U3-1402 showed HER3-specific binding followed by highly efficient cancer cell internalization. Subsequently,

U3-1402 was translocated to the lysosome and released its payload DXd. While U3-1402 was able to inhibit HER3-activated signaling similar to its naked antibody patritumab, the cytotoxic activity of U3-1402 in HER3-expressing cells was predominantly mediated by released DXd through DNA damage and apoptosis induction. In xenograft mouse models, U3-1402 exhibited dose-dependent and HER3-dependent antitumor activity. Furthermore, U3-1402 exerted potent antitumor activity against PDX tumors with HER3 expression. Acceptable toxicity was noted in both rats and monkeys.

Conclusions: U3-1402 demonstrated promising antitumor activity against HER3-expressing tumors with tolerable safety profiles. The activity of U3-1402 was driven by HER3-mediated payload delivery via high internalization into tumor cells.

Introduction

HER3 (ErbB3) is a member of the HER family, and its overexpression is frequently observed in various cancers (1). Unlike other HER family molecules, HER3 has a feature of lacking or having minimal intrinsic kinase activity (2–4), but it can be phosphorylated by forming a heterodimer with other receptor tyrosine kinases such as HER2. Dimerization of HER3 induced by ligand binding or overexpression of dimer partners activates the intracellular signaling pathways, mainly the PI3K/AKT pathway and MAPK/ERK pathway (1, 5), which promote several biological

responses, such as cell survival and proliferation, ultimately leading to tumor progression (5–8). Activation of the PI3K/AKT pathway is also thought to be a major cause of treatment failure in cancer therapy because of its role in drug resistance (9, 10).

According to a recent meta-analysis, HER3 overexpression might be associated with poor prognosis in solid tumors, including breast, gastric, and ovarian cancers and melanoma (11). These findings support the importance of developing an effective therapy targeting HER3 to overcome treatment failure and to improve treatment outcome in patients with cancer. Considering the lack of appreciable kinase activity in HER3, antibodies have been the main modality to target HER3 through mechanisms such as blocking the interaction of HER3/ligands or HER3/other-HER receptors, and engaging the immune system for cancer cell killing. In fact, there are a number of HER3-targeting antibodies under preclinical evaluation and clinical development (12). Although pertuzumab, a HER2-targeting antibody which inhibits the dimerization of HER2 with other HER family receptors including HER3, is clinically available for patient with HER2-positive breast cancer, to date, no HER3-targeting antibody has been approved for clinical use because of the limited evidence of clinical benefit. Therefore, further effective strategies are required for HER3-targeting therapy.

¹Daiichi Sankyo Co., Ltd., Tokyo, Japan. ²National Institute of Biomedical Innovation, Health and Nutrition, Osaka, Japan.

Note: Supplementary data for this article are available at Clinical Cancer Research Online (<http://clincancerres.aacrjournals.org/>).

Corresponding Author: Yasuki Kamai, Daiichi Sankyo Co., Ltd., 1-2-58 Hiromachi, Shinagawa-ku, Tokyo 140-8710, Japan; Phone: 813-3492-3131; Fax: 813-5436-8578; E-mail: kamai.yasuki.n2@daiichisankyo.co.jp

Clin Cancer Res 2019;25:7151-61

doi: 10.1158/1078-0432.CCR-19-1745

©2019 American Association for Cancer Research.

Translational Relevance

HER3, one of the HER family molecules, is highly expressed in various tumor types. It is believed to play essential roles in cancer pathogenesis, thus many anti-HER3 antibodies have been developed for cancer treatment. However, to date, none of them has shown satisfactory efficacy in clinical trials. In this preclinical study, we produced U3-1402, an anti-HER3 antibody–drug conjugate consisting of a novel linker and potent topoisomerase I inhibitor exatecan derivative (DXd), to treat HER3-expressing tumors. U3-1402 shows HER3-specific binding with highly efficient internalization into tumor cells. After linker cleavage, U3-1402 induces tumor cells to undergo apoptosis through DNA damage via released DXd. U3-1402 exhibits potent and dose-dependent antitumor activity in xenograft models compared with naked antibody in a HER3-dependent manner with acceptable toxicity. Altogether, our findings emphasize the potential efficacy of U3-1402 as a first-in-class treatment option for patients with HER3-expressing cancers.

Antibody–drug conjugate (ADC) is one of the promising treatment modalities to potentially increase the effectiveness and reduce off-target systemic toxicity. It can exhibit potent antitumor activity with a wide therapeutic window by utilizing the advantage of the specificity of an antibody to deliver potent cytotoxic drugs into tumor cells. The mechanisms of action of ADCs are generally thought to be as follows: after binding of the ADC to the cell surface antigen, the ADC–antigen complex undergoes internalization and translocation to the lysosomal compartment where the ADC is degraded to release the payload drug, which causes cell death (13).

We engineered U3-1402, a novel HER3-targeting ADC, which comprises patritumab (U3-1287), a fully human anti-HER3 mAb, linked to a potent topoisomerase I inhibitor (exatecan derivative: DXd) via a peptidyl linker, using our original technology (14, 15). As our linker-payload technology enables a stable and high (8 DXds per antibody) drug-to-antibody ratio (DAR) without compromising the physicochemical properties, U3-1402 is expected to steadily deliver DXds to the HER3-expressing tumors. The utility of our linker-payload technology has been demonstrated in [fam]-trastuzumab deruxtecan (T-DXd, DS-8201a), a novel HER2-targeting ADC, which has been reported to show potent antitumor activity in various tumor xenograft models (16, 17) and promising efficacy in patients with cancer (18). Patritumab, the antibody part of U3-1402, is an antibody against the extracellular domain of HER3, and has been shown to inhibit ligand-induced phosphorylation of HER3 and to suppress tumor growth in some tumor xenograft models (19, 20). In addition, in clinical trials, it was well-tolerated and showed some evidence of therapeutic activity (21, 22). Given that U3-1402 has the features of patritumab and HER3-specific delivery of DXd, it could be a promising treatment option for HER3-expressing cancers.

In this article, we describe the preclinical profiles of U3-1402, including its mechanisms of action and antitumor activity. U3-1402 has potent and HER3-dependent antitumor activity mainly by the action of topoisomerase I inhibitor delivered via efficient drug internalization.

Materials and Methods

Antibodies and ADCs

U3-1402 was synthesized in accordance with the published procedure (14, 15), conjugating the exatecan derivative-based cytotoxic payload with the naked anti-HER3 antibody (patritumab, U3-1287). Using matched isotype mAb, control IgG-ADC was synthesized in the same manner as U3-1402, resulting in a comparable DAR. Anti-HER2 mAb was produced with the same amino acid sequence as trastuzumab, demonstrating high binding affinity and specificity to the extracellular domain of HER2.

Cell lines

The human breast cancer cell lines HCC1569, SK-BR-3, MDA-MB-453, MDA-MB-361, MDA-MB-231, and MDA-MB-175VII, and human cervical cancer C-33A were purchased from ATCC. The human breast cancer cell line JIMT-1 was purchased from Leibniz Institute DSMZ, and the human ovarian cancer cell line OVCAR8 was from the NIH. HCC1569, SK-BR-3, MDA-MB-231, CFPAC-1, JIMT-1, C-33A, and OVCAR8 were cultured with appropriate media (RPMI1640-ATCC medium for HCC1569, McCoy 5A Medium for SK-BR-3, RPMI1640 for MDA-MB-231 and OVCAR8, and DMEM for JIMT-1) supplemented with 10% FBS at 37°C and a 5% CO₂ atmosphere. MDA-MB-453, MDA-MB-361, and MDA-MB-175VII were cultured with Leibovitz L-15 medium supplemented with 10% FBS (15% FBS for MDA-MB-361) at 37°C in a free gas exchange with atmospheric air.

ELISA

Flat 96-well immunoplates were coated with 2 µg/mL His-tagged human HER family recombinant proteins, EGFR, HER2, HER3, and HER4 (Sino Biological Inc.), overnight at 4°C, washed, blocked with 1% BSA, and then incubated with 10 µg/mL U3-1402 or IgG-ADC for 1 hour at 37°C. Anti-His and isotype control antibodies were also used as positive and negative controls, respectively. After washing, horseradish peroxidase (HRP)-conjugated anti-human IgG antibody (Jackson ImmunoResearch Laboratories, Inc.) was added and incubated for another hour, followed by washing and the addition of 3,3',5,5'-tetramethylbenzidine soluble reagent (ScyTek Laboratories, Inc.). The absorbance at 450 nm was measured using a microplate reader, SpectraMax M3 (Molecular Devices, LLC).

Flow cytometry

The detached HCC1569 and C-33A cells were stained with FITC-conjugated anti-HER3 antibody or FITC-conjugated control IgG (Miltenyi Biotec GmbH) on ice for 45 minutes in the dark. Washed cells were analyzed using the flow cytometer BD FACS-Calibur (Becton, Dickinson and Company).

Cytotoxic assay under three-dimensional culture conditions

Cells (1×10^3 cells/well) were seeded in PrimeSurface 96U plates (Sumitomo Bakelite Co., Ltd.), cultured for 3 days for sphere formation, and then treated with a serial dilution of DXd and U3-1402. After 7 days of incubation, cell viability was measured by CellTiter-Glo Reagent (Promega Corp.) using the luminometer Micro Beta TRILUX (PerkinElmer Co., Ltd.). IC₅₀ was calculated by the Sigmoid Emax model with SAS9.1.3 (SAS Institute Japan Ltd.).

Binding and internalization assay

Cells were seeded in 24-well plates at $1.5\text{--}3.5 \times 10^5$ cells/well. After overnight culture, cells were treated with U3-1402 and IgG-ADC (10 $\mu\text{g}/\text{mL}$) for 0.5, 1, 3, and 6 hours at 37°C for internalization assay. After detaching the adherent cells by treatment with cell dissociation buffer (Life Technologies), cells were stained with secondary antibody, Alexa Fluor 647 goat anti-human IgG (Thermo Fisher Scientific, 10 $\mu\text{g}/\text{mL}$), and incubated on ice for 1 hour in the dark. The cells were fixed with paraformaldehyde (Wako) for 20 minutes and analyzed by a flow cytometer, Attune NxT (Thermo Fisher Scientific). For the detection of cell surface binding, cells were incubated on ice for 1 hour with each test substance. Cell surface binding was expressed in mean fluorescence intensity (MFI), and internalization percent was calculated from the MFI reduction from the cell surface using the following equation: $100 - (\text{MFI of treated cells at } 37^\circ\text{C}/\text{MFI of treated cells on ice}) \times 100$. Both patritumab and anti-HER2 mAb (10 $\mu\text{g}/\text{mL}$) were additionally tested in a certain cell line.

Trafficking assay

U3-1402 and IgG-ADC were labeled with a pH-sensitive dye, pHrodo, using pHrodo iFL Red Microscale Protein Labeling Kit (Thermo Fisher Scientific) by incubation for 1 hour in 10 mmol/L acetate/5% sorbitol, pH 5.5 (Nacalai), and then purified with zeba-spin Desalting Column (Thermo Fisher Scientific) and Amicon Ultra-0.5 (Merck-Millipore). Cells were seeded in a 96-well plate (CellCarrier-96 Ultra, PerkinElmer) at 5×10^4 cells/well. After overnight culture, cells were treated with each pHrodo-labeled substance (10 $\mu\text{g}/\text{mL}$), along with Hoechst 33342 (100 ng/mL). Bright-field and fluorescence emission images were collected at 30-minute intervals for up to 12 hours, using a 403 confocal Opera Phoenix high-content screening system (PerkinElmer).

Payload determination

Cells were seeded in 24-well plates at 1.5×10^5 cells/well. After overnight culture, cells were treated with each test substance in a manner similar to that described in "binding and internalization assay." At 3, 6, and 24 hours, culture medium was collected and subjected to payload determination by an LC/MS-MS system consisting of API 5000 (AB SCIEX) coupled to an Agilent 1200 Series (Agilent Technologies), using Accucore RP-MS (2.1 \times 100 mm, 2.6 μm ; Thermo Fisher Scientific) as an analytical column (23).

Growth inhibition assay

Cells were seeded in black clear-bottomed 96-well plates at 1,000–2,000 cells/well. After overnight culture, each diluted test substance was added. After treatment for 6 days, cell viability was measured by the ATPlite one-step luminescence assay system, using EnVision multimode plate reader (PerkinElmer).

Western blotting

Cells were lysed in RIPA buffer supplemented with protease and phosphatase inhibitors (Thermo Fisher Scientific). The lysates were collected after centrifugation at 15,000 rpm for 20 minutes at 4°C , and then quantified for protein concentration using BCA Protein Assay (Thermo Fisher Scientific). Equal amounts of proteins were subjected to SDS-PAGE and transferred to polyvinylidene difluoride membranes (Bio-Rad Laboratories, Inc.). Immunoblot analyses were performed for pHER3

(Tyr1289), HER3, pAKT (Ser473), AKT, pERK1/2 (Thr202/Tyr204), ERK1/2, pChk1 (Ser317), Chk1, cPARP, PARP, pH2AX (Ser139), and β -actin. All primary antibodies and HRP-conjugated secondary antibodies used were purchased from Cell Signaling Technology, Inc. The membranes were incubated with Immobilon Forte Western HRP Substrate (Merck-Millipore) and visualized using the luminescent image analyzer LAS-4000 (FUJIFILM Corp.).

Xenograft studies

Cell line–derived xenograft (CDX) or patient-derived xenograft (PDX) models were established in athymic nude mice or SCID mice as described in Supplementary Materials and Methods. When the tumor volume reached approximately 100–300 mm^3 for CDX models or 200–400 mm^3 for PDX models, the tumor-bearing mice were assigned to the control and treatment groups, and dosing was started (day 0). U3-1402 was administered intravenously once on day 0 or once a week for 3 weeks, and then tumor volume defined as $1/2 \times \text{length} \times \text{width}^2$ was measured twice a week. The antitumor activity was evaluated approximately 3 weeks after initial administration, where tumor growth inhibition (TGI, %) was calculated according to the formula of $100 \times [1 - (\text{average tumor volume of the treatment group})/(\text{average tumor volume of the control group})]$, and tumor volumes were compared between control and treatment groups. All animal experiments performed in this study were approved by the Institutional Animal Care and Use Committee at Daiichi Sankyo Co., Ltd.

IHC and microscopy

Excised xenograft tumors were formalin-fixed and paraffin-embedded, and 4- μm tissue sections were used for IHC. See Supplementary Materials and Methods for further information.

Toxicity studies in rats and monkeys

U3-1402 was intravenously administered at 3-week intervals for a total of 12 weeks to CrI:CD(SD) rats or cynomolgus monkeys. Clinical signs, body weight, food consumption, and clinical pathology were monitored throughout the study. Necropsy was performed on the day after the last administration. The reversibility of the toxic changes was assessed in a subsequent 6-week recovery period in both rats and monkeys.

Results

HER3-targeting ADC U3-1402

U3-1402 is an ADC comprising the fully human anti-HER3 monoclonal IgG1 antibody patritumab, tetra-peptide based linker, and an exatecan-derivative topoisomerase I inhibitor DXd (Fig. 1A). Patritumab was conjugated with our linker-payload system, which is designed to be cleaved by lysosomal enzymes resulting in release of the payload DXd. Theoretically, eight cysteine residues of antibody are available for linker conjugation. Hydrophobic interaction chromatography showed a homogeneous drug distribution and the DAR of synthesized U3-1402 was observed to be approximately eight (Fig. 1B). To confirm the target specificity of U3-1402, we assessed its binding activity against human HER family proteins. The results of ELISA revealed that U3-1402 bound to human HER3 recombinant proteins; however, there was no binding detected against other human HER family proteins EGFR, HER2, and HER4 (Fig. 1C).

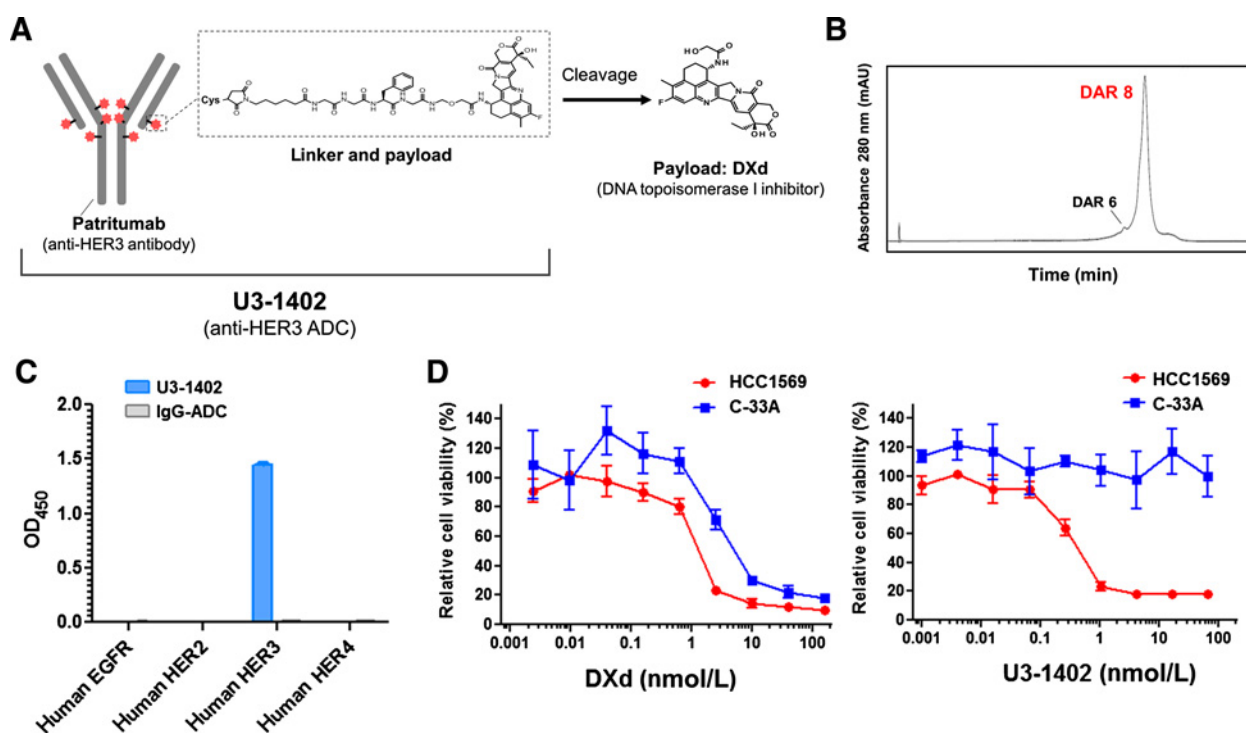


Figure 1. Structure and HER3-specific activity of U3-1402. **A**, Schematic structure of U3-1402. **B**, Conjugated drug distribution by hydrophobic interaction chromatography. **C**, Binding activity of U3-1402 against human HER family proteins. Recombinant proteins were incubated with U3-1402 or drug-conjugated control IgG (IgG-ADC), and bound antibodies were measured by ELISA. **D**, Cytotoxic activity of DXd and U3-1402. Cells were cultured under sphere culture conditions and treated with DXd or U3-1402 at the indicated concentrations for 7 days.

Furthermore, the cytotoxic activity of U3-1402 was evaluated under three-dimensional cell culture conditions using HER3-positive human cancer HCC1569 and HER3-negative human cancer C-33A cells (Supplementary Fig. S1A). Both HCC1569 and C-33A cells were susceptible to DXd with IC₅₀ of 1.3 nmol/L and 4.2 nmol/L, respectively. On the other hand, U3-1402 markedly decreased cell viability in only HCC1569 cells with IC₅₀ of 0.4 nmol/L (Fig. 1D), indicating that U3-1402 exerts HER3-dependent cytotoxic activity.

Molecular dynamics of U3-1402, patritumab, and anti-HER2 mAb

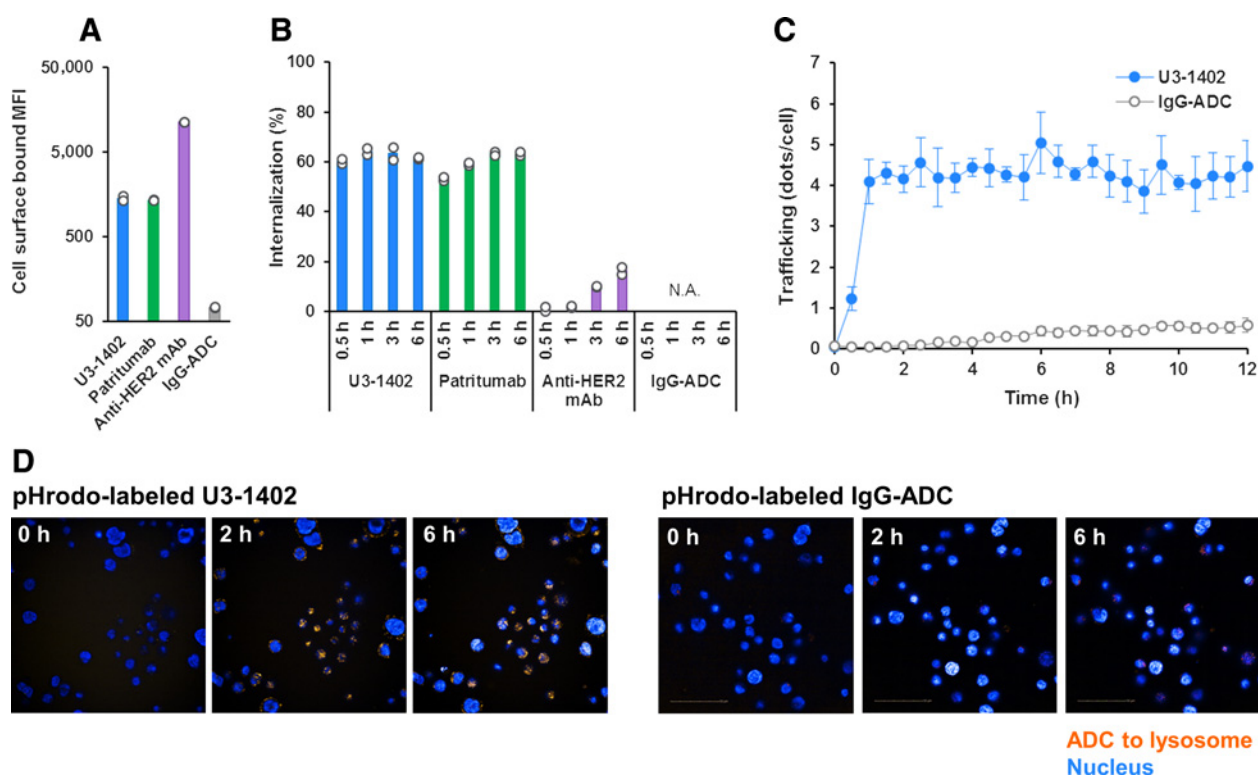
Cell surface binding and internalization were compared among U3-1402, patritumab, and anti-HER2 mAb in MDA-MB-453 cell line, which expresses both HER2 and HER3 (Supplementary Fig. S1B), using IgG-ADC as a control. U3-1402 bound to the cell surface at a higher level than IgG-ADC (Fig. 2A), and was then internalized into the cells (Fig. 2B). The binding and internalization levels of U3-1402 were quite similar to those of patritumab, indicating that these processes are dominantly mediated by the antibody component of U3-1402 with little or no effect from the linker-payload conjugate. U3-1402 had a binding level one-eighth of that of anti-HER2 mAb (Fig. 2A). However, U3-1402 was efficiently internalized into cells with a higher internalization rate than anti-HER2 mAb, reaching 64.1% and 1.7% at 1 hour for U3-1402 and anti-HER2 mAb, respectively (Fig. 2B). Thereafter, the internalized U3-1402 was translocated to the lysosome, which

was traced by monitoring pHrodo probe label-derived orange dots, more than IgG-ADC (Fig. 2C and D). This trafficking phenomenon was in good accordance with the binding and internalization of tested antibodies, where U3-1402 showed considerably high binding and internalization levels compared with IgG-ADC (Fig. 2A and B).

HER3-mediated molecular dynamics of U3-1402 in eight cancer cell lines

To assess the targeted delivery potential of U3-1402, cell surface binding, internalization, trafficking, and payload release were investigated in eight cancer cell lines with various HER3 expression levels, along with cell growth inhibition activity. Among all of the data obtained for internalization, trafficking, and payload release, the mean values at 6 hours were representatively plotted against cell surface binding level, as shown in Fig. 3A–C. U3-1402 bound to the cell surface in HER3-positive cell lines (HCC1569, SK-BR-3, MDA-MB-175VII, MDA-MB-453, MDA-MB-361, OVCAR-8, and JIMT-1), but not in the HER3-negative cell line MDA-MB-231 (Fig. 3A). In accordance with the cell surface binding levels, U3-1402 was internalized into cells at an average rate of 53.3% among the cell lines tested (Fig. 3A). The internalized U3-1402 was translocated to the lysosome (Fig. 3B), leading to DXd release (Fig. 3C). Overall, each of these intracellular processes tended to be correlated with the surface binding level, although MDA-MB-175VII tended to be an outlier in the linear regression (Fig. 3A–C).

Downloaded from <http://aacrjournals.org/clinccancerres/article-pdf/25/23/7151/20545227/7151.pdf> by Rockefeller University user on 08 March 2026

**Figure 2.**

Efficient internalization and trafficking properties of U3-1402 in MDA-MB-453 cells. **A** and **B**, Cell surface binding and internalization. The cells were treated with U3-1402, patritumab, anti-HER2 mAb, and IgG-ADC on ice for 1 hour (cell surface binding) and at 37°C for 0.5, 1, 3, and 6 hours (internalization). Each value represents the mean (closed bar) combined with individual values (open symbol) of duplicate samples. N.A., not applicable. **C**, Intracellular trafficking. The cells were treated with pHrodo-labeled U3-1402 and IgG-ADC, and the number of pHrodo-derived dots was measured up to 12 hours. Each point represents the mean and SD from triplicate samples. **D**, Time-lapse image of intracellular trafficking. pHrodo (orange) works as an acidic pH sensor, allowing discrimination of stages in the endocytosis pathway from early endosome to lysosome. Cells were counterstained with Hoechst 33342 (blue, nuclei).

In an *in vitro* antitumor test, growth inhibition activity was analyzed upon 6 days of treatment with U3-1402, patritumab, IgG-ADC, and DXd. Among the HER3-positive cell lines, U3-1402 showed cell growth inhibition activity against MDA-MB-453, HCC1569, SK-BR-3, and MDA-MB-175VII, but little or no activity against OVCAR-8, JIMT-1, and MDA-MB-361 (Supplementary Fig. S2). No cell growth inhibition of U3-1402 was observed in the HER3-negative cell line MDA-MB-231. There was a good correlation between relative cell viability at 10 nmol/L and the cell surface binding, with a correlation coefficient of -0.892 (95% confidence interval, -0.504 to -0.980 ; Fig. 3D). On the other hand, payload sensitivity was varied among the cell lines, showing the lowest sensitivity in JIMT-1 and MDA-MB-361, and the highest sensitivity in HCC1569 and MDA-MB-453; this might also have contributed to the varying growth inhibition activity of U3-1402 (Supplementary Fig. S2). Patritumab showed cell growth inhibition activity only against MDA-MB-175VII [endogenously neuregulin (NRG)-secreting cell line; ref. 24], not against the other seven cell lines, suggesting that signal inhibition might be responsible for the cell growth inhibition in this cell line (Supplementary Fig. S2). At the highest concentration (100 nmol/L) of U3-1402, HER3-independent cell growth inhibition activity was observed in the majority of the cell lines, based on the result that IgG-ADC had cell growth inhibition activity at this concentration (Supplementary Fig. S2).

HER3 signal inhibition and induction of DNA damage and apoptosis by U3-1402

Because patritumab blocks NRG-induced activation of HER3 and its downstream pathway (19, 20), we examined whether U3-1402 is capable of inhibiting HER3-mediated signaling. NRG-1, a high-affinity ligand of HER3, induced the phosphorylation of HER3, AKT, and ERK (Fig. 4A). These phosphorylations were clearly inhibited by U3-1402 as well as patritumab in all four cancer cell lines tested (Fig. 4A). In addition, decreases in total HER3 protein expression were also observed in the cells treated with both patritumab and U3-1402 (Fig. 4A). To verify the contribution of payload drug to the cytotoxic activity of U3-1402, we next analyzed the phosphorylation of Chk1 and H2AX, DNA damage markers, and PARP cleavage, a marker of apoptosis, which are known to be induced by topoisomerase I inhibitors (16). Although intrinsic HER3/AKT activation was diminished by both patritumab and U3-1402, increased phosphorylation of Chk1 and H2AX was induced by only U3-1402 in MDA-MB-453, HCC1569, and SK-BR-3 cells (Fig. 4B). In these cell lines, cleaved PARP was detected in cells treated with U3-1402 for 72 hours. In MDA-MB-175VII cells, both patritumab and U3-1402 caused PARP cleavage after 6 hours of treatment, whereas no obvious changes in phosphorylated Chk1 (Fig. 4B) and H2AX (data not shown) were observed. Collectively, our results imply that

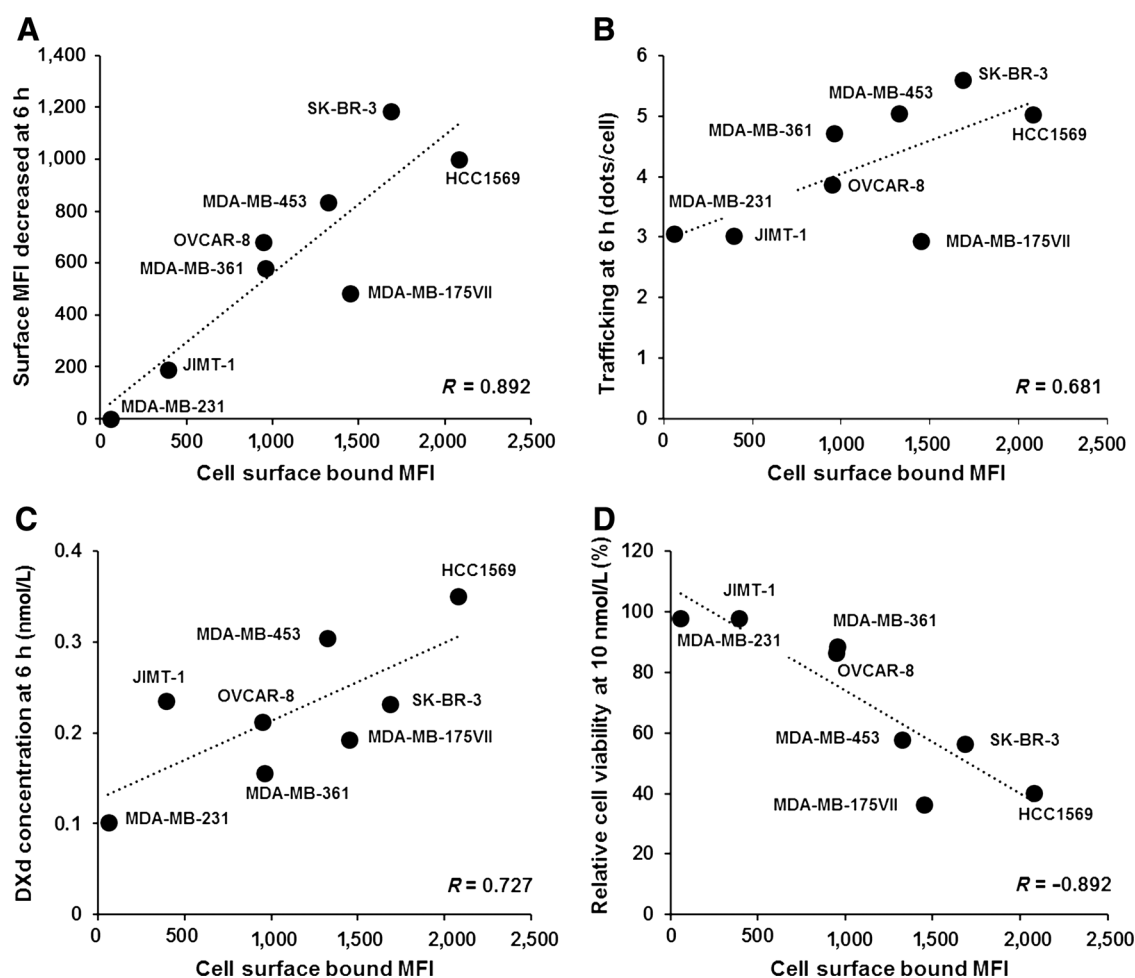


Figure 3. Correlation between cell surface binding of U3-1402 and its subsequent intracellular processes in eight cell lines with different HER3 expression levels. **A–C,** Plots of the correlations of internalization, trafficking, and DXd release with the cell surface binding of U3-1402. Each intracellular dynamic value at 6 hours was chosen as a representative and plotted against cell surface binding with a correlation coefficient. **D,** Plots of the correlation of cell growth inhibitory activity with cell surface binding of U3-1402. Relative cell viability under treatment with 10 nmol/L U3-1402 for 6 days was chosen as a representative and plotted against cell surface binding with a correlation coefficient.

U3-1402 inhibits HER3-mediated signaling, but also induces apoptosis, attributable mainly to payload activity.

In vivo antitumor activity of U3-1402

To determine whether U3-1402 exerts antitumor activity *in vivo*, we used a human breast cancer cell line MDA-MB-453 xenograft model, featuring tumors with high HER3 expression (Fig. 6B). Mice bearing tumors were administered intravenously with an escalating dose of U3-1402 at 0.375, 0.75, 1.5, 3, and 6 mg/kg. The treatment with U3-1402 at 0.75, 1.5, 3, and 6 mg/kg significantly inhibited tumor growth with TGI indices of 45%, 68%, 82%, and 94%, respectively, compared with the control group at 21 days after administration ($P < 0.001$; Fig. 5A). Next, to ascertain target-specific and payload-dependent activity of U3-1402, we evaluated the antitumor activity of U3-1402, patritumab, and IgG-ADC in an MDA-MB-453 xenograft model. While neither patritumab at 3 mg/kg nor IgG-ADC at 3 mg/kg inhibited the tumor growth, 3 mg/kg U3-1402 treatment led to significant tumor regression

with a TGI of 87% ($P < 0.001$; Fig. 5B). Moreover, this activity was clearly abolished by the preadministration of patritumab, indicating that HER3-binding competition diminished the effectiveness of U3-1402. Taken together, these results demonstrate the dose-dependent and HER3-specific *in vivo* antitumor activity of U3-1402.

Antitumor activity of U3-1402 in various xenograft models

To confirm the HER3-dependent effectiveness of U3-1402, the antitumor activity of U3-1402 was examined using HER3-positive CDX models and a HER3-negative CDX model. IHC showed HER3 expression in the membrane of tumor cells in HCC1569 (Fig. 6A) and MDA-MB-453 models (Fig. 6B), but not in MDA-MB-231 model (Fig. 6C). In these experiments, the mice were treated with 3 mg/kg U3-1402 (weekly, 3 times in total). In HER3-positive CDX models, U3-1402 showed potent and significant antitumor activity with TGI of 73% for HCC1569 and 95% for MDA-MB-453. In contrast, U3-1402 was not effective in the

Downloaded from <http://aacrjournals.org/clinccancerres/article-pdf/25/23/7151/2054522/7151.pdf> by Rockefeller University user on 08 March 2026

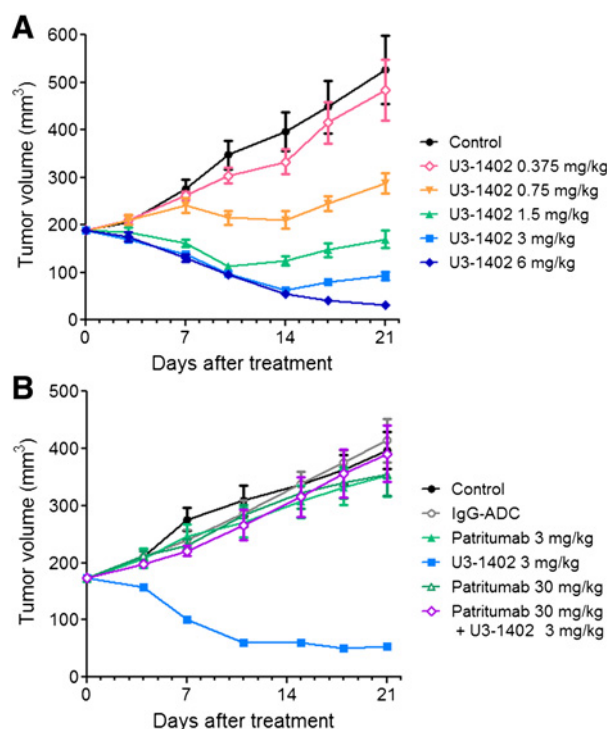


Figure 5. Antitumor activity of U3-1402 in HER3-positive human cancer MDA-MB-453 xenograft model. **A**, Mice inoculated with MDA-MB-453 cells were intravenously administered with vehicle control or U3-1402 at the indicated doses on day 0 ($n = 10$ mice/group). **B**, Mice with MDA-MB-453 xenograft were intravenously treated with 3 mg/kg U3-1402, 3 mg/kg IgG-ADC, 3 and 30 mg/kg patritumab, or 30 mg/kg patritumab followed by 3 mg/kg U3-1402 ($n = 6$ mice/group). Mean and SE of tumor volume are shown.

to 30 mg/kg, the highest dose tested. On the basis of the mortality and severity of the findings, the severely toxic dose of 10% in animals was considered to be 194 mg/kg for rats, and the highest nonseverely toxic dose for monkeys was considered to be 30 mg/kg. These toxicologic findings in animals with repeated administrations suggest acceptable safety profiles of U3-1402.

Discussion

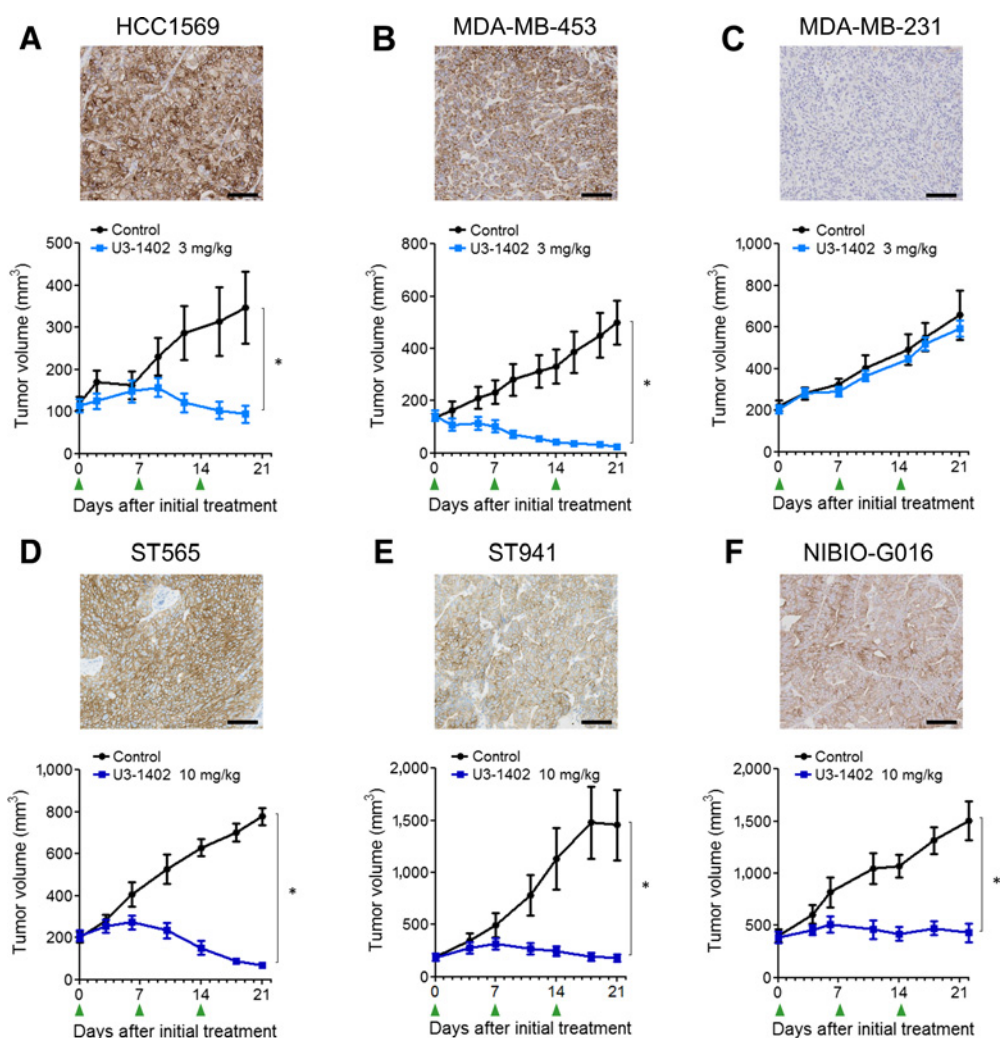
ADC is a promising modality for cancer therapy, as evidenced by the regulatory approval and clinical use of several ADCs, such as brentuximab vedotin (CD30-targeting ADC), trastuzumab emtansine (HER2-targeting ADC), and inotuzumab ozogamicin (CD22-targeting ADC; refs. 13, 26). HER3 has long been considered as an attractive target due to its critical role in tumor development and prognosis, as well as its expression in a variety of malignant tumors; however, no therapeutic agents targeting HER3 directly have been approved to date (12, 27). Here, we engineered a novel HER3-targeting ADC, U3-1402, and demonstrated its HER3-specific and payload drug-derived antitumor activity in preclinical cancer models.

A number of mAbs against HER3 have been developed and shown to inhibit HER3 downstream signaling pathways, through preventing ligand binding, blocking dimerization with other HER family members, locking HER3 in an inactive conformation, and/or triggering HER3 internalization (12, 27). U3-1402 is generated

on the basis of a HER3-targeting mAb, patritumab, which blocks ligand binding and induces HER3 internalization, thereby attenuating HER3-mediated signaling (19, 20). Despite linker-payload conjugation, U3-1402 retained these mAb properties similar to patritumab. Among eight cancer cell lines tested in this study, however, patritumab inhibited cell growth in only MDA-MB-175VII cells in which both patritumab and U3-1402 induced PARP cleavage, but not DNA damage markers. Because MDA-MB-175VII cells have been reported to secrete NRG in an autocrine manner (24), NRG/HER3 signal blockade is likely a predominant mechanism of cell growth inhibition by patritumab and U3-1402 in this cell line. In contrast, U3-1402 did exert cytotoxic activity in other cell lines, including MDA-MB-453, HCC1569, and SK-BR-3 cells. In these cell lines, U3-1402 caused DNA damage followed by PARP cleavage, suggesting the cytotoxic activity resulting from topoisomerase I inhibitor DXd. In addition, while patritumab did not show antitumor activity, U3-1402 significantly inhibited tumor growth in the MDA-MB-453 xenograft model. Other mechanisms that might contribute to the antitumor activity of mAb-based therapy are antibody-dependent cellular cytotoxicity (ADCC) and complement-dependent cytotoxicity (CDC; ref. 27). However, U3-1402 exhibited neither ADCC nor CDC activity (data not shown). Our results suggest that U3-1402 instead exerts antitumor activity not only by inhibiting HER3-mediated signaling but also through payload activity. Although multiple clinical trials for mAb-based HER3 therapy have been completed or are currently ongoing, there has been no regulatory approval because of the limited clinical benefit in these trials. It is hoped that a HER3-targeting ADC approach would overcome the limitations of mAb-based HER3 therapy, with potent and broad antitumor activity.

The mechanism of action of ADC involves several processes, including (i) binding to target, (ii) antibody internalization, (iii) intracellular trafficking, and (iv) payload release (13, 28), all of which appear to contribute to the efficacy of ADC therapy. Our data presented here demonstrate the HER3-specific binding, lysosome translocation following internalization, and payload DXd release of U3-1402. Intriguingly, U3-1402 was efficiently internalized into cells at an average rate of over 50%. This internalization rate was higher than that of anti-HER2 mAb, even though the expression level of cell surface HER3 was lower than that of HER2. This finding is consistent with a previous report (29). As recent studies have identified several molecules responsible for HER3 internalization (30–33), it would be important to elucidate the factors impacting on U3-1402 internalization, which are currently being studied. The U3-1402 internalization, lysosome translocation, and released DXd concentration tended to be positively correlated with U3-1402 binding to cell surface HER3. Decreases in total HER3 expression in U3-1402-treated cells observed by Western blot analysis may indicate degradation of the HER3–U3-1402 complex during intracellular processes. More importantly, *in vitro* cell growth inhibition by U3-1402 was also associated with cell surface binding, suggesting the HER3-dependent drug delivery ability of U3-1402. However, as noted earlier, varied sensitivity of tumor cells to topoisomerase I inhibitors might be a confounding factor to define the antitumor activity of U3-1402.

We utilized PDX models as well as CDX mouse models to evaluate *in vivo* antitumor activity. U3-1402 significantly inhibited tumor growth and even led to tumor regression in tumors with HER3 expression, but not in HER3-negative tumor. Our

**Figure 6.**

Antitumor activity of U3-1402 in xenograft models. **A**, Breast cancer CDX with HCC1569. **B**, Breast cancer CDX with MDA-MB-453. **C**, Breast cancer CDX with MDA-MB-231. **D**, Breast cancer PDX with ST565. **E**, Breast cancer PDX with ST941. **F**, Gastric cancer PDX with NIBIO-G016. Representative images of tumors stained for HER3 by IHC are shown for each model. Scale bar, 100 μ m. Arrowhead indicates the administration point. Each point represents the mean and SE ($n = 4-10$). *, statistically significant difference compared with the control ($P < 0.01$) analyzed by Student t test.

results from *in vitro* and *in vivo* studies verified that HER3 expression is crucial for the antitumor activity of U3-1402. However, given the heterogeneity and complexity of tumors, careful consideration and biomarker selection might be necessary to stratify patients who will benefit from U3-1402 treatment.

The majority of ADCs under development and used clinically have DAR of 2–4, as ADCs with a DAR higher than 6 are thought to have decreased efficacy and increased toxicity due to the instability of linker and conjugation chemistry (26, 34). Nonetheless, our linker-payload technology enables ADC to carry eight molecules of payload (DAR 8) with improved stability and uniformity, which has been demonstrated in [fam-] trastuzumab deruxtecan (T-DXd, formerly DS-8201a; ref. 16), an anti-HER2 ADC comprising the same linker and payload as U3-1402. Similar to DS-8201a, the plasma exposure level of DXd was negligible in animals treated with U3-1402 (data not shown), therefore min-

imal toxicity was expected. In toxicity studies, a few severe toxicologic findings typical of topoisomerase I inhibitors were observed. Bensch and colleagues have investigated whole-body distribution of anti-HER3 antibody lumretuzumab in patients with solid tumors by PET imaging and reported that relatively high tracer uptake was observed in liver and intestine (35). However, few toxicologic findings of U3-1402 in these organs were found in rats or cynomolgus monkeys. As such, the overall safety profiles of U3-1402 in animal models suggest that U3-1402 would be well-tolerated as an anticancer agent. On the basis of preclinical evaluations described partly here, phase I clinical trials of U3-1402 are currently ongoing in metastatic breast cancer (ClinicalTrials.gov identifier: NCT02980341) and in non-small cell lung cancer (ClinicalTrials.gov identifier: NCT03260491). Preliminary results from these clinical trials showed an acceptable safety profile and promising antitumor activity of U3-1402 (36, 37).

HER3 is also known to play a pivotal role in drug resistance. Accumulating evidence indicates that the increased HER3 expression and/or activation are associated with resistance to various anticancer therapeutics, such as EGFR- and HER2-targeted therapies and hormonal therapies (38–40). In fact, recent work demonstrated that U3-1402 is effective in EGFR tyrosine kinase inhibitor (TKI)-resistant tumors and exhibits enhanced antitumor activity against these tumors by combining with an EGFR-TKI (41), suggesting further potential of U3-1402 and a rationale for applying a combinatorial strategy in cancer treatment.

In summary, U3-1402 demonstrated potent antitumor activity against HER3-expressing tumors through HER3-specific payload delivery via efficient intracellular internalization. U3-1402 may offer a promising treatment option for patients with HER3-expressing tumors.

Disclosure of Potential Conflicts of Interest

Y. Hashimoto, K. Koyama, Y. Kamai, K. Hirotsu, Y. Ogitani, A. Zembutsu, M. Abe, Y. Kaneda, N. Maeda, Y. Shiose, T. Iguchi, T. Ishizaka, T. Karibe, K. Morita, T. Nakada, K. Wakita, T. Kagari, Y. Abe, M. Murakami, S. Ueno, and T. Agatsuma are employees/paid consultants for Daiichi Sankyo Co., Ltd. I. Hayakawa reports receiving commercial research grants from Daiichi Sankyo Co., Ltd. No potential conflicts of interest were disclosed by the other authors.

Authors' Contributions

Conception and design: Y. Hashimoto, Y. Shiose, K. Morita, M. Murakami, S. Ueno, T. Agatsuma

Development of methodology: Y. Ogitani, A. Zembutsu, M. Abe, Y. Kaneda, T. Ishizaka, I. Hayakawa, K. Morita, T. Nomura, S. Ueno

Acquisition of data (provided animals, acquired and managed patients, provided facilities, etc.): Y. Hashimoto, K. Koyama, Y. Kamai, K. Hirotsu, Y. Ogitani, A. Zembutsu, M. Abe, Y. Kaneda, T. Iguchi, T. Ishizaka, T. Karibe, K. Morita, S. Ueno

Analysis and interpretation of data (e.g., statistical analysis, biostatistics, computational analysis): Y. Hashimoto, K. Koyama, Y. Kamai, K. Hirotsu, Y. Ogitani, A. Zembutsu, N. Maeda, T. Ishizaka, M. Murakami, S. Ueno

Writing, review, and/or revision of the manuscript: Y. Hashimoto, K. Koyama, Y. Kamai, Y. Ogitani, A. Zembutsu, Y. Shiose, T. Ishizaka, I. Hayakawa, T. Nakada, K. Wakita, M. Murakami, T. Agatsuma

Administrative, technical, or material support (i.e., reporting or organizing data, constructing databases): Y. Kamai, T. Ishizaka, T. Nakada, T. Agatsuma

Study supervision: K. Wakita, T. Kagari, Y. Abe, S. Ueno, T. Agatsuma

Other (establishment of suitable PDX model): T. Nomura

Acknowledgments

The authors thank Birgit Frankenberger, Sabine Blum, Reimar Abraham, and Akira Okubo for their technical assistance. They also thank all of the members who provided their expertise and assistance in the preclinical studies.

The costs of publication of this article were defrayed in part by the payment of page charges. This article must therefore be hereby marked *advertisement* in accordance with 18 U.S.C. Section 1734 solely to indicate this fact.

Received May 28, 2019; revised July 30, 2019; accepted August 27, 2019; published first August 30, 2019.

References

- Campbell MR, Amin D, Moasser MM. HER3 comes of age: new insights into its functions and role in signaling, tumor biology, and cancer therapy. *Clin Cancer Res* 2010;16:1373–83.
- Boudeau J, Miranda-Saavedra D, Barton GJ, Alessi DR. Emerging roles of pseudokinases. *Trends Cell Biol* 2006;16:443–52.
- Citri A, Skaria KB, Yarden Y. The deaf and the dumb: the biology of ErbB-2 and ErbB-3. *Exp Cell Res* 2003;284:54–65.
- Shi F, Telesco SE, Liu Y, Radhakrishnan R, Lemmon MA. ErbB3/HER3 intracellular domain is competent to bind ATP and catalyze autophosphorylation. *Proc Natl Acad Sci USA* 2010;107:7692–7.
- Olayioye MA, Neve RM, Lane HA, Hynes NE. The ErbB signaling network: receptor heterodimerization in development and cancer. *EMBO J* 2000;19:3159–67.
- Baselga J, Swain SM. Novel anticancer targets: revisiting ERBB2 and discovering ERBB3. *Nat Rev Cancer* 2009;9:463–75.
- Hynes NE, MacDonald G. ErbB receptors and signaling pathways in cancer. *Curr Opin Cell Biol* 2009;21:177–84.
- Yarden Y, Sliwkowski MX. Untangling the ErbB signalling network. *Nat Rev Mol Cell Biol* 2001;2:127–37.
- Amin DN, Campbell MR, Moasser MM. The role of HER3, the unpretentious member of the HER family, in cancer biology and cancer therapeutics. *Semin Cell Dev Biol* 2010;21:944–50.
- Knuefermann C, Lu Y, Liu B, Jin W, Liang K, Wu L, et al. HER2/PI-3K/Akt activation leads to a multidrug resistance in human breast adenocarcinoma cells. *Oncogene* 2003;22:3205–12.
- Ocana A, Vera-Badillo F, Seruga B, Templeton A, Pandiella A, Amir E. HER3 overexpression and survival in solid tumors: a meta-analysis. *J Natl Cancer Inst* 2013;105:266–73.
- Mishra R, Patel H, Alanazi S, Yuan L, Garrett JT. HER3 signaling and targeted therapy in cancer. *Oncol Rep* 2018;12:355.
- Parslow A, Parakh S, Lee F-T, Gan H, Scott A. Antibody–drug conjugates for cancer therapy. *Biomedicines* 2016;4:14.
- Ogitani Y, Abe Y, Iguchi T, Yamaguchi J, Terauchi T, Kitamura M, et al. Wide application of a novel topoisomerase I inhibitor-based drug conjugation technology. *Bioorg Med Chem Lett* 2016;26:5069–72.
- Nakada T, Masuda T, Naito H, Yoshida M, Ashida S, Morita K, et al. Novel antibody drug conjugates containing exatecan derivative-based cytotoxic payloads. *Bioorg Med Chem Lett* 2016;26:1542–5.
- Ogitani Y, Aida T, Hagihara K, Yamaguchi J, Ishii C, Harada N, et al. DS-8201a, a novel HER2-targeting ADC with a novel DNA topoisomerase I inhibitor, demonstrates a promising antitumor efficacy with differentiation from T-DM1. *Clin Cancer Res* 2016;22:5097–108.
- Ogitani Y, Hagihara K, Oitate M, Naito H, Agatsuma T. Bystander killing effect of DS-8201a, a novel anti-human epidermal growth factor receptor 2 antibody–drug conjugate, in tumors with human epidermal growth factor receptor 2 heterogeneity. *Cancer Sci* 2016;107:1039–46.
- Doi T, Shitara K, Naito Y, Shimomura A, Fujiwara Y, Yonemori K, et al. Safety, pharmacokinetics, and antitumor activity of trastuzumab deruxtecan (DS-8201), a HER2-targeting antibody–drug conjugate, in patients with advanced breast and gastric or gastro-oesophageal tumours: a phase 1 dose-escalation study. *Lancet Oncol* 2017;18:1512–22.
- Kawakami H, Okamoto I, Yonesaka K, Okamoto K, Shibata K, Shinkai Y, et al. The anti-HER3 antibody patritumab abrogates cetuximab resistance mediated by heregulin in colorectal cancer cells. *Oncotarget* 2014;5:11847–56.
- Yonesaka K, Hirotsu K, Kawakami H, Takeda M, Kaneda H, Sakai K, et al. Anti-HER3 monoclonal antibody patritumab sensitizes refractory non-small cell lung cancer to the epidermal growth factor receptor inhibitor erlotinib. *Oncogene* 2016;35:878–86.
- LoRusso P, Janne PA, Oliveira M, Rizvi N, Malburg L, Keedy V, et al. Phase I study of U3-1287, a fully human anti-HER3 monoclonal antibody, in patients with advanced solid tumors. *Clin Cancer Res* 2013;19:3078–87.
- Wakui H, Yamamoto N, Nakamichi S, Tamura Y, Nokihara H, Yamada Y, et al. Phase 1 and dose-finding study of patritumab (U3-1287), a human monoclonal antibody targeting HER3, in Japanese patients with advanced solid tumors. *Cancer Chemother Pharmacol* 2014;73:511–6.
- Nagai Y, Oitate M, Shiozawa H, Ando O. Comprehensive preclinical pharmacokinetic evaluations of trastuzumab deruxtecan (DS-8201a), a HER2-targeting antibody–drug conjugate, in cynomolgus monkeys. *Xenobiotica* 2019;49:1086–96.

24. Schaefer G, Fitzpatrick VD, Sliwkowski MX. γ -Heregulin: a novel heregulin isoform that is an autocrine growth factor for the human breast cancer cell line, MDA-MB-175. *Oncogene* 1997;15:1385–94.
25. Pommier Y. Drugging topoisomerases: lessons and challenges. *ACS Chem Biol* 2013;8:82–95.
26. Beck A, Goetsch L, Dumontet C, Corvaia N. Strategies and challenges for the next generation of antibody–drug conjugates. *Nat Rev Drug Discov* 2017;16:315–37.
27. Jacob W, James I, Hasmann M, Weisser M. Clinical development of HER3-targeting monoclonal antibodies: Perils and progress. *Cancer Treat Rev* 2018;68:111–23.
28. Hedrich WD, Fandy TE, Ashour HM, Wang H, Hassan HE. Antibody-drug conjugates: pharmacokinetic/pharmacodynamic modeling, preclinical characterization, clinical studies, and lessons learned. *Clin Pharmacokinet* 2018; 57:687–703.
29. Hettmann T, Schneider M, Ogbagabriel S, Xie J, Juan G, Hartmann S, et al. U3-1287 (AMG 888), a fully human anti-HER3 mAb, inhibits HER3 activation and induces HER3 internalization and degradation [abstract]. In: Proceedings of the 101st Annual Meeting of the American Association for Cancer Research; 2010 Apr 17–21; Washington, DC. Philadelphia (PA): AACR; 2010. Abstract nr LB-306.
30. Qiu X-B, Goldberg AL. Nrdp1/FLRF is a ubiquitin ligase promoting ubiquitination and degradation of the epidermal growth factor receptor family member, ErbB3. *Proc Natl Acad Sci U S A* 2002;99:14843–8.
31. Huang Z, Choi B, Mujoo K, Fan X, Fa M, Mukherjee S, et al. The E3 ubiquitin ligase NEDD4 negatively regulates HER3/ErbB3 level and signaling. *Oncogene* 2015;34:1105–15.
32. Szymanska M, Fosdahl AM, Raiborg C, Dietrich M, Liestøl K, Stang E, et al. Interaction with epsin 1 regulates the constitutive clathrin-dependent internalization of ErbB3. *Biochim Biophys Acta* 2016;1863:1179–88.
33. Fosdahl AM, Dietrich M, Schink KO, Malik MS, Skeie M, Bertelsen V, et al. ErbB3 interacts with Hrs and is sorted to lysosomes for degradation. *Biochim Biophys Acta Mol cell Res* 2017;1864:2241–52.
34. Hamblett KJ, Senter PD, Chace DF, Sun MMC, Lenox J, Cervený CG, et al. Effects of drug loading on the antitumor activity of a monoclonal antibody drug conjugate. *Clin Cancer Res* 2004;10:7063–70.
35. Bensch F, Lamberts LE, Smeenk MM, Jorritsma-Smit A, Lub-de Hooge MN, Terwisscha van Scheltinga AGT, et al. ⁸⁹Zr-lumretuzumab PET imaging before and during HER3 antibody lumretuzumab treatment in patients with solid tumors. *Clin Cancer Res* 2017;23:6128–37.
36. Kogawa T, Yonemori K, Masuda N, Takahashi S, Takahashi M, Iwase H, et al. Single agent activity of U3-1402, a HER3-targeting antibody-drug conjugate, in breast cancer patients: phase 1 dose escalation study. *J Clin Oncol* 2018;36:2512.
37. Masuda N, Yonemori K, Takahashi S, Kogawa T, Nakayama T, Iwase H, et al. Single agent activity of U3-1402, a HER3-targeting antibody-drug conjugate, in HER3-overexpressing metastatic breast cancer: updated results of a phase 1/2 trial [abstract]. In: Proceedings of the 2018 San Antonio Breast Cancer Symposium; 2018 Dec 4–8; San Antonio, TX. Philadelphia (PA): AACR; 2019. Abstract nr PD1-03.
38. Yonesaka K, Zejnullahu K, Okamoto I, Satoh T, Cappuzzo F, Souglakos J, et al. Activation of ERBB2 signaling causes resistance to the EGFR-directed therapeutic antibody cetuximab. *Sci Transl Med* 2011;3: 99ra86.
39. Narayan M, Wilken JA, Harris LN, Baron AT, Kimbler KD, Maible NJ. Trastuzumab-induced HER reprogramming in "resistant" breast carcinoma cells. *Cancer Res* 2009;69:2191–4.
40. Morrison MM, Hutchinson K, Williams MM, Stanford JC, Balko JM, Young C, et al. ErbB3 downregulation enhances luminal breast tumor response to antiestrogens. *J Clin Invest* 2013;123:4329–43.
41. Yonesaka K, Takegawa N, Watanabe S, Haratani K, Kawakami H, Sakai K, et al. An HER3-targeting antibody-drug conjugate incorporating a DNA topoisomerase I inhibitor U3-1402 conquers EGFR tyrosine kinase inhibitor-resistant NSCLC. *Oncogene* 2019;38: 1398–409.